

## Preparation of a Cr coating on low-carbon steel by electrodeposition in a NaCl-KCl-NaF-Cr<sub>2</sub>O<sub>3</sub> molten salt

Shixian Zhang<sup>1,2</sup>, Yungang Li<sup>1,\*</sup>, Cong Wang<sup>1</sup>, Xiaoping Zhao<sup>2</sup>

<sup>1</sup> Key Laboratory of Ministry of Education for Modern Metallurgy Technology, College of Metallurgy and Energy, North China University of Science and Technology, Tangshan 063009, China;

<sup>2</sup> Hebei College of Industry and Technology, Shijiazhuang 050091, China;

\*E-mail: [liyungang59322@163.com](mailto:liyungang59322@163.com)

Received: 4 September 2018 / Accepted: 7 November 2018 / Published: 30 November 2018

The thermodynamic calculation results of electrochemical reduction in a NaCl–KCl–NaF–Cr<sub>2</sub>O<sub>3</sub> molten salt system indicates that it is feasible to prepare a Cr coating on low carbon steel by electrochemical deposition. The electrochemical reaction mechanism and electrocrystallization process of chromium investigated at 1073 K by an electrochemical workstation, indicate that the electrochemical reduction of Cr(III) to Cr takes two steps,  $\text{Cr}^{3+} + \text{e} \rightarrow \text{Cr}^{2+}$ , and  $\text{Cr}^{2+} + 2\text{e} \rightarrow \text{Cr}$ . The electrochemical processes of Cr(III) and Cr(II) are quasi-reversible reactions, and the electrocrystallization process of Cr is an instantaneous hemispheroid three-dimensional nucleation process. A Cr coating with thickness of 250 μm was successfully deposited on a low carbon steel substrate. The atomic growth process, composition and morphology of the coating were investigated by SEM, EDS and XRD. The results of the AC impedance method show that the corrosion resistance of the Cr-coated low-carbon steel is much higher than that of low-carbon steel.

**Keywords:** Thermodynamic calculation; Coating; Electrochemical deposition; Characterization

### 1. INTRODUCTION

Carbon-steel materials are recognized as the most widely used materials in engineering fields, such as construction, machinery manufacturing, and shipbuilding, because of their cheap, simple manufacturing process, good plasticity, toughness, and ease of machining. However, their poor corrosion resistance is an Achilles' heel for many applications in many field. It has been reported that the direct economic losses caused by corrosion is approximately 1.5 ~ 4.2% of Europe's GNP[1], and people tolerate close to 700 yuan of corrosion damage per year in China[2].

In order to solve this important problem, scholars have proposed the idea of preparing protective

coatings for carbon-steel surfaces[3-5], which aimed to improve the corrosion resistance of carbon-steel materials with minimal investment[6-9]. Among the various metallic coatings, Fe-Cr alloy coatings have attracted wide attention. They are widely used in the fields of nuclear power systems, solid fuel cells and high-temperature structural materials, due to their low cost, strong corrosion resistance[10,11], high boiling point, high hardness, and especially their high-temperature and magnetic properties.

In this paper, a Cr coating on a low-carbon steel substrate surface prepared by the molten salt electrodeposition method is proposed for the first time. The electrochemical reduction and nucleation mechanism of Cr (III) in a NaCl–KCl–NaF–Cr<sub>2</sub>O<sub>3</sub> molten salt were studied. Then, Cr-coated low-carbon steel was prepared via electrochemical deposition. Its corrosion resistance was studied by electrochemical testing.

## 2. EXPERIMENTAL

### 2.1 Theoretical calculation

The thermodynamic data of the molten salt electrochemical reduction were calculated using HSC7.0 software, which was designed by Outokumpu Research Oy in Finland.

### 2.2 Materials

All of the analytically- pure reagents were weighed with a molar ratio of  $X_{\text{NaCl}}:X_{\text{KCl}}:X_{\text{NaF}}:X_{\text{Cr}_2\text{O}_3} = 0.64:0.64:0.32:0.01$  and mixed. The mixed salt was ground with an agate mortar and heated at 473 K for 12 hours.

### 2.3 Electrocrystallization

The dried reagents were placed in a high-purity zirconia crucible and placed in a resistance furnace. The furnace temperature was controlled by an artificial intellectual controller (Model: AI-808p) and measured by a thermocouple (Model: S) with an accuracy of  $\pm 1$  °C. The furnace was airtight so that the experiment could be performed in an inert atmosphere of high-purity argon gas. The NaCl-KCl-NaF and NaCl-KCl-NaF-Cr<sub>2</sub>O<sub>3</sub> molten salts were isothermally maintained for 7 hours at 1073 K.

Pre-electrolysis was performed for 2 hours at a constant voltage of 2 V to remove residual water, oxide anions, and other compounds. The molten salt electrochemistry experiment was carried out by a Zahner workstation (Model: IM6eX, Germany) using a traditional three-electrode cell configuration. The reference and counter electrodes were made of platinum wire with a diameter of 0.5 mm (99.99%). The working electrode was made of low-carbon steel wire with a diameter of 0.5 mm. Alumina tubes with an inner diameter of 0.6 mm were used as the sleeve. The three electrodes were soaked in concentrated hydrochloric acid for 1 minute and shaken with an ultrasonic cleaner containing deionized water and ethanol for 5 minutes. They were dried with a blower before each experiment. The CV curves of NaCl-KCl-NaF and NaCl-KCl-NaF-Cr<sub>2</sub>O<sub>3</sub> were measured using a scanning rate of 0.5 V/s at 1073 K.

The CV curves of NaCl-KCl-NaF-Cr<sub>2</sub>O<sub>3</sub> were measured between the scanning rates 0.3 and 0.6 V/s (step of 0.1 V/s) at 1073 K. The chronoamperometry curves of the NaCl-KCl-NaF-Cr<sub>2</sub>O<sub>3</sub> molten salt were measured in the potential range of -0.3 to -0.35 V.

#### 2.4 Electrodeposition

According to the results of the electrochemical experiments, low-carbon steel sheets (wC=0.20%, wMn=0.24%, wP=0.03%, wS=0.02%, and wSi=0.11%) were used as the electrochemical deposition substrate with dimensions of 20 mm×20 mm×1 mm. The low-carbon steel sheet electrodes were polished with silicon carbide sandpaper (320, 500, 1000, 1500, and 2000 mesh) and then degreased by immersion in a 5% NaOH solution for 5 minutes. The electrodes were soaked in a 5% hydrochloric acid solution for 5 minutes, rinsed in an ultrasonic cleaner for 5 minutes with ethanol, and then blown dry for later electrodeposition experiments. The electrodeposition experiments were performed on the low-carbon steel sheet substrate in NaCl-KCl-NaF-Cr<sub>2</sub>O<sub>3</sub> molten salt at 1073 K with a current density of 300 mA/cm<sup>2</sup> and deposition times of 30 minutes or 6 hours.

#### 2.5 Analysis and detection

The surface morphology and chemical composition of the working electrode were observed by an FEI, Quanta, 650 FEG field emission scanning electron microscope and its auxiliary energy dispersive X-ray spectrometer (EDS). The phase composition of the substrate surface was tested by an X-ray diffractometer (D/MAX 2500 PC). The corrosion resistance of the Cr-coated low-carbon steel was determined by the AC impedance method at 25 °C in an aerated 3.5% NaCl aqueous solution.

### 3. RESULTS AND DISCUSSION

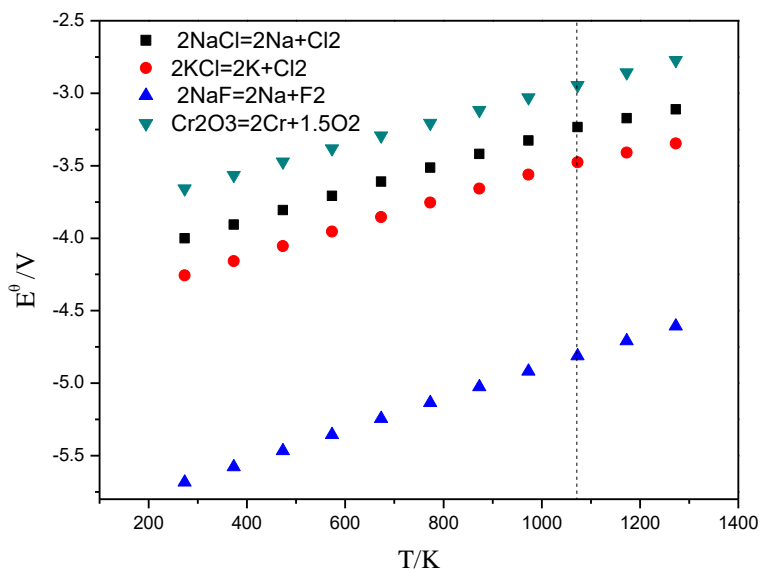
#### 3.1 Thermodynamic analysis

The theoretical decomposition voltages ( $E^\theta$ ) for the electrolytic reaction to pure metal were calculated by HSC thermodynamic 7.0 software according to the following formula (1)[11]:

$$\Delta G^\theta = -nFE^\theta \quad (1)$$

where  $\Delta G^\theta$  is the standard Gibbs free energy change (kJ/mol),  $n$  is the electron transfer number and  $F$  is Faraday's constant (96485 C/mol).

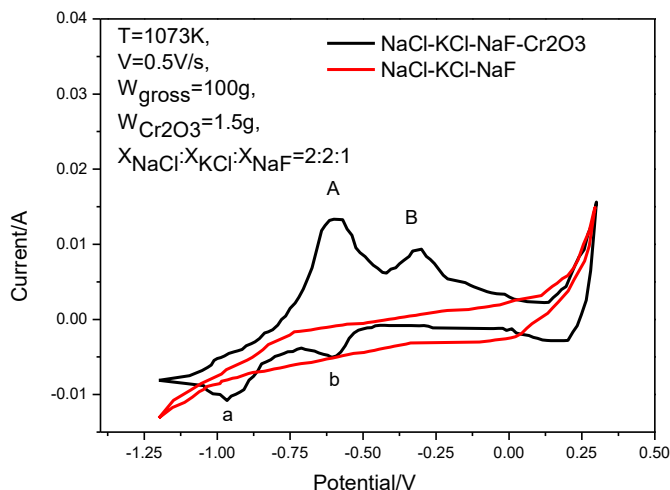
As shown in Fig. 1, the theoretical decomposition voltages of NaCl, KCl and NaF are -3.23, -3.48 and -4.81 V at 1073 K, respectively. However, the theoretical decomposition voltage of Cr<sub>2</sub>O<sub>3</sub> to obtain pure metal is only -2.94 V at 1073 K. This value is much lower than that of NaCl, KCl and NaF. Hence, the electrochemical reduction of Cr<sub>2</sub>O<sub>3</sub> into pure metal in a NaCl-KCl-NaF-Cr<sub>2</sub>O<sub>3</sub> molten salt is thermodynamically feasible[12].



**Figure 1.** The theoretical decomposition voltages of NaCl, KCl, NaF and Cr<sub>2</sub>O<sub>3</sub>

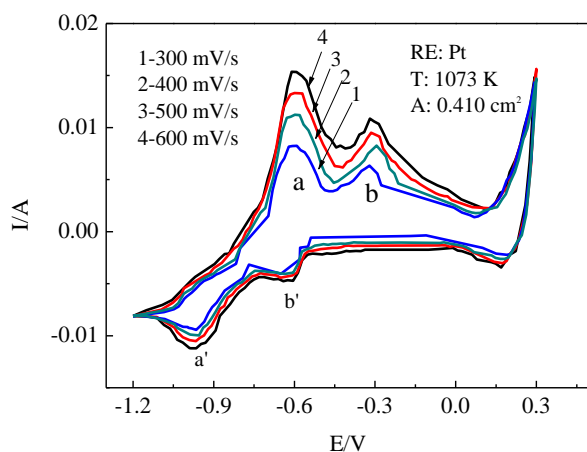
### 3.2 Cyclic voltammetry

Fig. 2 shows the typical CV curves obtained on a low-carbon steel electrode in a NaCl-KCl-NaF molten salt with and without Cr<sub>2</sub>O<sub>3</sub> at 1073 K. Since there are double electron layers in the redox process, the starting point for measuring the peak current is not the zero-current line. The red curve displays the voltammogram of the NaCl-KCl-NaF molten salt. This voltammogram reveals that no redox reaction occurs between -1.2 and 0.3 V because no cathodic/anodic peak appears. This result was verified in another paper[13]. In contrast, the black curve presents the voltammogram of the molten salt with Cr<sub>2</sub>O<sub>3</sub>. Two pairs of cathodic/anodic (A/a and B/b) peaks are observed, which correspond to the deposition and dissolution of Cr. The result is similar to Xiangzhu He's[14]. This result probably indicates that Cr(III) is reduced to metallic Cr through two steps in an electron transfer reaction. Peak b in the negative-direction scan corresponds to the transformation of Cr(III) to Cr(II), while peak a corresponds to the transformation of Cr(II) to Cr. Correspondingly, peaks A and B in the positive-direction scan represent the dissociation of Cr into Cr(II) and Cr(II) to Cr(III), respectively. This is in agreement with the studies of Giovanardi[15].



**Figure 2.** Typical CV curves of NaCl-KCl-NaF and NaCl-KCl-NaF-Cr<sub>2</sub>O<sub>3</sub> at 1073 K

The typical CV curves of the NaCl–KCl–NaF–Cr<sub>2</sub>O<sub>3</sub> molten salt were measured at different scanning rates between -1.2 and 0.3 V, as shown in Fig. 3. The peaks of a/a’ and b/b’ represent the reduction/oxidation processes of Cr(II) and Cr(III) on the cathodic/anodic electrodes, respectively. They appear at almost the same voltage. The potential difference for the redox reaction increases with increasing scanning rate. To validate the reversibility of the cathodic reduction process, discharge steps and electron transfer number, hidden data from the reduction peaks a’ and b’ were extracted and calculated.



**Figure 3.** Typical CV curves of the electrochemical reaction in a molten salt system at different scanning rates

Fig. 4 depicts the relationship between the current density ( $i_{pc}$ ) and the scan rate square root ( $v^{1/2}$ ) of reduction peaks a’ and b’. It can be seen that both reduction peaks have a nearly linear relation, but neither of the two lines passes through the origin of the coordinate system. Therefore, it can be concluded that the reactions of Cr(III) and Cr(II) are quasi-reversible reactions in the NaCl–KCl–NaF–Cr<sub>2</sub>O<sub>3</sub> molten salt. The reduction of Cr(III) is controlled by the rate of electroactive ion diffusion, indicating that the product on the cathodic electrode is insoluble through  $|i_{pa} / i_{pc}| > 1$ [16].

Assuming that the reduction process on the electrode is reversible and that the product is insoluble, the experimental data can be used in equation  $\phi_{pc} - \phi_{pc/2} = -0.77 (RT/nF)$ [17,18], which can be used as the criterion to judge the reversibility of the corresponding electrochemical reaction ( $\phi_{pc/2}$  is the half-peak potential). The results show that the electron transfer number of reduction peak a' is 2, while the electron transfer number of reduction peak b' is 1. Therefore, it can be concluded that the reduction of  $\text{Cr}^{3+}$  to Cr during electrochemical reduction takes place in two steps:  $\text{Cr}^{3+} + e \rightarrow \text{Cr}^{2+}$  and  $\text{Cr}^{2+} + 2e \rightarrow \text{Cr}$ .

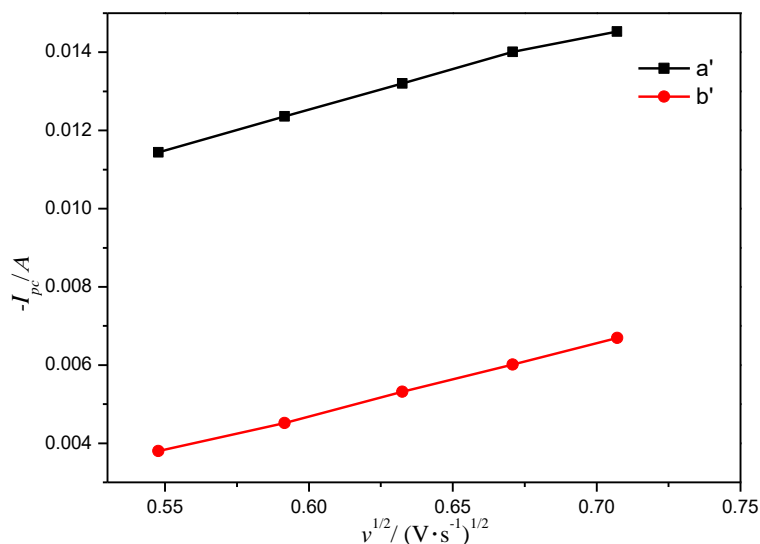


**Figure 4.** Relationship between  $I_{pc}$  and  $v^{1/2}$  for peaks a' and b'

### 3.4 Chronoamperometry

The electrochemical formation of a Cr coating on low-carbon steel via Cr deposition was measured by chronoamperometry. The curves in Fig. 5 show the typical features of a reduction process controlled by planar diffusion. The different stages of the curve represent the different nucleation processes of Cr during electrocrystallization. The double electron layer is charged at the moment of potential application.  $\text{Cr}^{3+}$  is reduced to a Cr-crystal nucleus when the current is stepped at the beginning. After that, the Cr-nuclei concentration increases with a decrease in the Cr-ion concentration and the formation of Cr nuclei before 0.1 s. The current starts to decrease between 0.1 and 0.7 s because of the concentration polarization that occurs on the cathode surface at the same time. Afterwards, the current stabilizes as the nucleus begins to grow, and no new nuclei are formed[19].

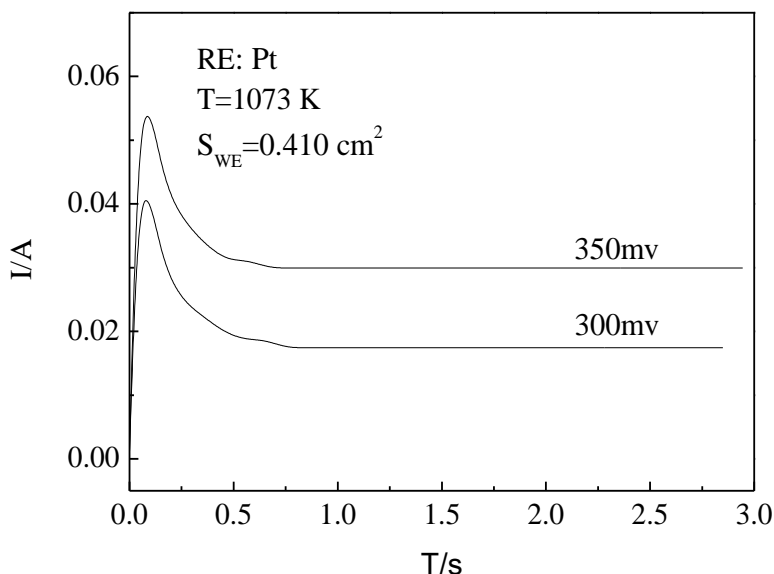


**Figure 5.** Chronoamperometry curve of Cr electrochemical reduction

The implicit data from the chronoamperogram at 350 mV in Fig. 5 were extracted and calculated[19]. The relationship between  $I-t^{1/2}$  and  $I-t^{3/2}$  of the chronoamperogram is shown in Fig. 6. After performing linear regression on the data, the results of the regression equations are as follows:

$$I = 1.04366 - 0.1621t^{1/2}, R^2=0.997 \tag{2}$$

$$I = 0.9625 - 0.900t^{3/2}, R^2=0.962 \tag{3}$$

It is found that the goodness of fit for liner regression equation (2) is better than the observation. Therefore, it is confirmed that the electrocrystallization process of Cr in a NaCl–KCl–NaF–Cr<sub>2</sub>O<sub>3</sub> molten salt is an instantaneous hemispheroid three-dimensional nucleation process[20].

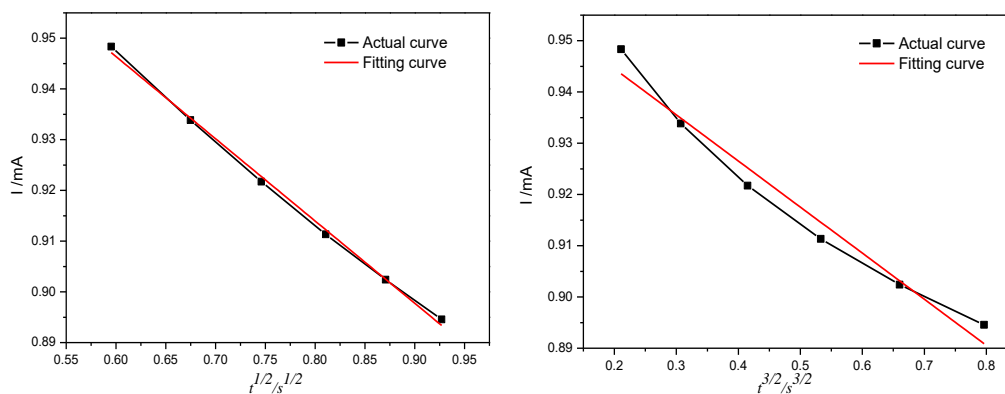


**Figure 6.** Relationship between  $I\sim t^{1/2}$  (a) and  $I\sim t^{3/2}$  (b) in the chronoamperogram at 350mV in Figure 5

### 3.5 Constant current electrolysis and characterization of a Cr coating on low-carbon steel

The deposition process was performed in a NaCl–KCl–NaF–Cr<sub>2</sub>O<sub>3</sub> molten salt at 1073 K for 30 minutes using a constant current density of 300 mA/cm<sup>2</sup>. The phase composition of the substrate surface was measured by XRD and is shown in Fig. 7. The validated chromium and iron peaks appear on the substrate surface. The surface of the substrate was imaged and is shown in Fig. 8. It can be seen that approximately 2 μm hemispherical three-dimensional nuclei particles are randomly attached to the

surface of the substrate, and the content of Cr is 26.74%. This suggests that chromium can be reduced by electrochemical methods.

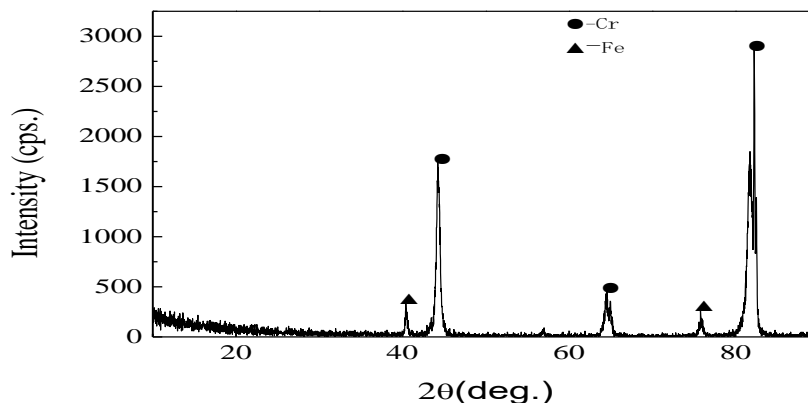


**Figure 7.** XRD pattern of the Cr coating on a low-carbon steel substrate deposited at 1073 K for 30 minutes

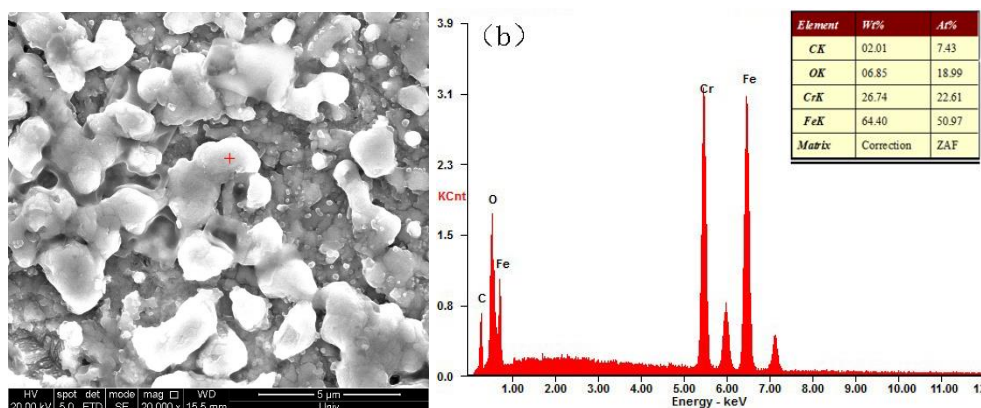


**Figure 8.** SEM image and EDS results for the Cr coating deposited on a low-carbon steel substrate at 1073 K for 30 minutes

Additionally, the deposition process was performed in a NaCl–KCl–NaF–Cr<sub>2</sub>O<sub>3</sub> molten salt at 1073 K for 6 hours using a constant current density of 300 mA/cm<sup>2</sup>. The SEM images of the original and polished substrate cross section are shown in Fig. 9. The columnar crystals closely adhere to the surface of the matrix. An approximately 250 μm thick Cr coating, which was uniform, and smooth, with tiny, regular grains, was deposited on the substrate.

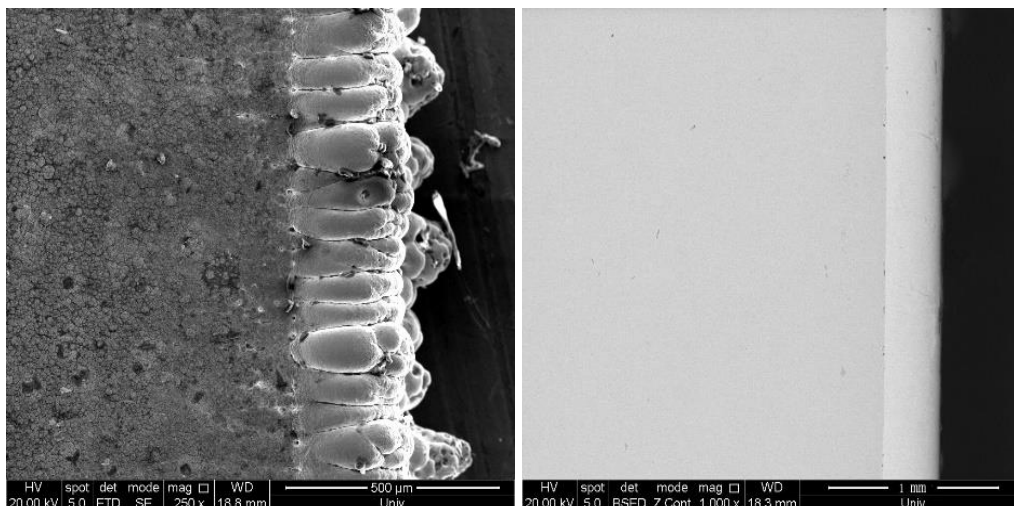


**Figure 9.** Cross-sectional SEM images of the Cr coating deposited on a low-carbon steel substrate at 1073 K for 6 hours

3.6 Corrosion resistance of the low carbon steel substrate and Cr-coated low-carbon steel

Fig. 10 shows the Nyquist diagram measured by the AC impedance method. It can be seen that the impedance radius of the Cr-coated low carbon steel is much larger than that of the low-carbon steel. This difference means that the corrosion resistance of the Cr-coated low-carbon steel is much higher than that of low-carbon steel[21].

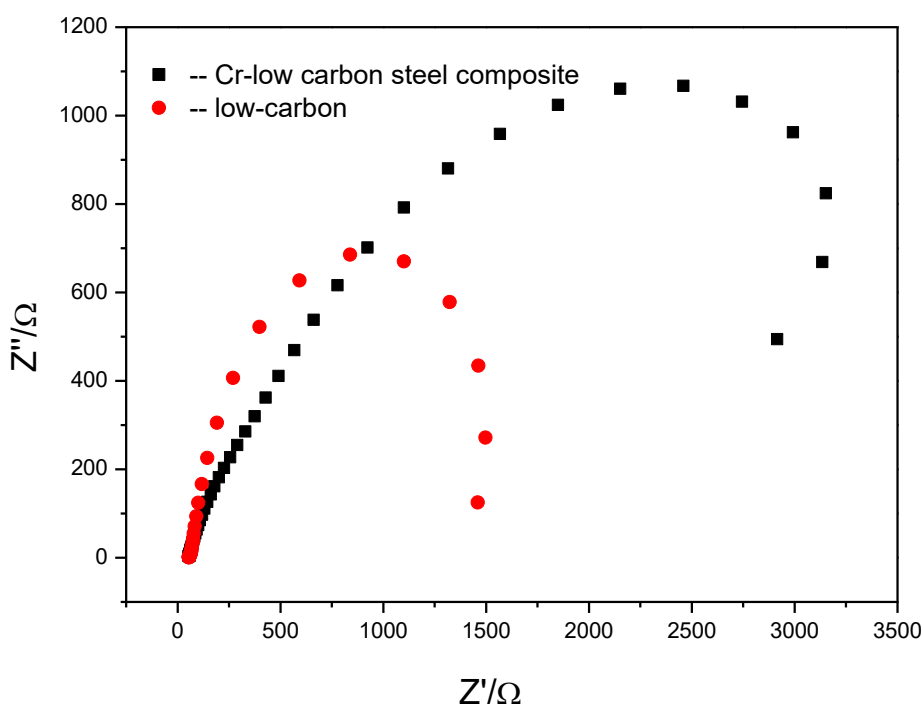


**Figure 10.** Nyquist diagram of Cr-coated low-carbon steel and low-carbon steel in a 3.5% NaCl solution

#### 4. CONCLUSION

The electrochemical reduction mechanism and deposition behaviour of Cr on a low carbon steel substrate in a NaCl–KCl–NaF–Cr<sub>2</sub>O<sub>3</sub> molten salt was investigated at 1073 K. According to the studies, the reduction of Cr(III) to Cr during electrochemical reduction occurs in two steps,  $\text{Cr}^{3+} + e \rightarrow \text{Cr}^{2+}$  and  $\text{Cr}^{2+} + 2e \rightarrow \text{Cr}$ . The electrochemical reaction of Cr(III) and Cr(II) is a quasi-reversible reaction controlled by the rate of electroactive ion diffusion. The electrocrystallization process of Cr is an instantaneous hemispheroid three-dimensional nucleation process. A compact, uniform Cr coating of 250  $\mu\text{m}$  was successfully prepared via electrochemical deposition. The corrosion resistance of the Cr-coated low-carbon steel is much higher than that of low-carbon steel.

#### ACKNOWLEDGEMENTS

The study is financially supported by the National Natural Science Foundation of China (51474088) and the Hebei Province Natural Science Foundation (E2016209163).

#### References

1. James Nogara, Sadiq J. Zarrouk. *Renew. Sust. Energ. Rev.*, 82 (2018) 1347.
2. Xiaohu Luo, Xinyu Pan, Song Yuan, Shuo Du, Caixia Zhang and Yali Liu. *Corros. Sci.*, 15 (2017) 139.
3. Toto Sudiro, April Imelda Juita Hia, Ciswandi, DidikAryanto, Bambang Hermanto, Agus Sukarto Wismogroho and Perdamean Sebayang. *J. Alloy. Compd.*, 732 (2018) 655.
4. N. K. Manninen, S. Calderón V., C. F. Alves, Almeida Alves, S. Carvalho and A. Cavaleiro. *Surf. Coat. Tech.*, 275 (2015) 127.
5. G. Y. Fu, L. Q. Wei, X. M. Zhang, Y. B. Cui, C. C. Lv, J. Ding, B. Yu and S. F. Ye. *Surf. Coat. Tech.*, 310 (2017) 166.
6. X. J. Lu, Z. D. Xiang. *Surf. Coat. Tech.*, 309 (2017) 994.
7. Yangshuhan Xu, Mingyan Liu. *Geothermics*, 70 (2017) 339.
8. Chengdong Chen, Shigang Dong, Ruiqing Hou, Juan Hu, Pingli Jiang, Chenqing Ye, Ronggui Du and Changjian Lin. *Surf. Coat. Tech.*, 326 (2017) 183.
9. Linqing Niu, Ruiguang Guo, Changbing Tang, Hongtao Guo and Jie Chen. *Surf. Coat. Tech.*, 300 (2016) 110.
10. Jie Wu, Bin Wang, Yifan Zhang, Run Liu, Yuan Xia, Guang Li and Wenbin Xue. *Mater. Chem. Phys.*, 171 (2016) 50.
11. Xiaohui Ye, Zhe Lin, Hongjun Zhang, Hongwei Zhu, Zhu Liu and Minlin Zhong. *Carbon*, 94 (2015) 326.
12. A. J. Bard, L.R. Faulkner. *Electrochemical Methods - Fundamentals and Applications*, Second Edition. *John Wiley Sons, Inc.*, (2001) New York.
13. Shixian Zhang, Yungang Li, Kai Hu, Xiaoping Zhao, Hui Li and Jinglong Liang. *Int. J. Electrochem. Sci.*, 13 (2018) 8030.
14. Xiangzhu He, Zhuqing Gong, Hanying Jiang. *T. Nonferr. Metal. Soc.*, 10 (2000) 95
15. R. Giovanardi, G. Orlando. *Surf. Coat. Tech.*, 205 (2011) 3947.
16. D.D. Macdonald. *Transient Techniques in Electrochemistry*. *Plenum Press*, (1981) New York.
17. J Wang. *Analytical Electrochemistry*, Third Edition. *Wiley-VCH*, (2006) Germany.
18. W Schmickler, E Santos. *Interfacial Electrochemistry*, Second Edition. *Springer*, (2010) Heidelberg.

19. A. K. Shukla, B. Hariprakash. Encyclopedia of Electrochemical Power Sources. *Elsevier Science Publishing Co. Inc.*, (2009) Netherlands.
20. Yuekun Gu, Jie Liu, Shengxiang Qu, Yida Deng, Xiaopeng Han, Wenbin Hu and Cheng Zhong. *J. Alloy. Compd.*, 690 (2017) 228.
21. Xin Shu, Yuxin Wang, Chuming Liu, Abdullah Aljaafari and Wei Gao. *Surf. Coat. Tech.*, 261(2015) 161.

© 2019 The Authors. Published by ESG ([www.electrochemsci.org](http://www.electrochemsci.org)). This article is an open access article distributed under the terms and conditions of the Creative Commons Attribution license (<http://creativecommons.org/licenses/by/4.0/>).